MODELING THE PHOTODEGRADATION OF TRACE ORGANIC COMPOUNDS IN RECLAIMED WASTEWATER FOR UV-185/254 NM CONTINUOUS-FLOW PHOTOREACTOR

by

Jordan Thomas

A Thesis Submitted to the Faculty of the

DEPARTMENT OF CHEMICAL AND ENVIRONMENTAL ENGINEERING

In Partial Fulfillment of the Requirements

For the Degree of

MASTER OF SCIENCE

In the Graduate College

THE UNIVERSITY OF ARIZONA

2025

THE UNIVERSITY OF ARIZONA
GRADUATE COLLEGE

As members of the Master's Committee, we certify that we have read the thesis prepared by Jordan Thomas, titled: *Modeling the Photodegradation of Trace Organic Compounds in Reclaimed Wastewater for UV-185/254 nm Continuous Flow Photoreactor* and recommend that it be accepted as fulfilling the dissertation requirement for the Master's Degree.

A. Eduardo Sáez Date: 04/25/2025

Robert G. Arnold Date: 04/25/2025

David M. Quanrud Date: 04/25/2025

Final approval and acceptance of this thesis is contingent upon the candidate's submission of the final copies of the thesis to the Graduate College.

I hereby certify that I have read this thesis prepared under my direction and recommend that it be accepted as fulfilling the Master's requirement.

A. Eduardo Sáez Date: 04/25/2025
Master's Thesis Committee Chair
Department of Chemical & Environmental Engineering

TABLE OF CONTENTS

LIST OF FIGURES

LIST OF TABLES

ABSTRACT

With the perpetually growing demands for potable water due to climate change, population growth, and urbanization, reclaimed wastewater is increasingly important as a source of potable water. Reclaimed wastewater must undergo intensive treatment to meet drinking water standards. Contaminants resistant to conventional treatment methods such as trace organic compounds (TOrCs) pose significant risks to human health even at low concentrations. Some TOrCs that resist conventional wastewater treatment can be removed through a combination of direct and indirect photolysis under UV-254 nm irradiation. Experiments were conducted for twenty-one TOrCs to determine photodegradation kinetics associated with UV-254 nm light. Quantum yields were determined for each TOrC and successfully used to model the photodegradation of each in reclaimed wastewater in both batch and continuous-flow reactor systems.

1 INTRODUCTION

Potable water scarcity issues are becoming increasingly concerning as access to freshwater due to ever increasing global demand. In a recent assessment on water availability within the United States, the U.S. Geological Survey (USGS) found that almost 30 million Americans live with large limitations on water usage (Castro-Lindarte, 2025). Around half of the world's population experiences severe water scarcity for at least a portion of the year (IPCC, 2023). To combat global water scarcity and keep up with ever-growing water demands, wastewater reclamation for potable reuse is necessary to ensure basic needs can be met.

Reuse water treated via conventional methods is can be used for municipal and industrial purposes. However, more rigorous treatment methods are required to meet drinking water requirements due to resistant contamination including many trace organic compounds (TOrCs). TOrCs include an extensive group of organic chemicals including pesticides, pharmaceuticals, and personal care products that generally exist in wastewater at low concentrations relative to other contaminants (Wie et al., 2016).

Well established processes for the removal of some TOrCs include ozone-based or UV irradiation-based advance oxidation processes (AOPs). In UV irradiation-based AOPs, hydrogen peroxide is commonly added to generate reactive radical species such as hydroxide radicals that oxidize TOrCs (Miklos et al., 2018). UV-based AOPs are becoming increasingly common within treatment systems due to more stringent EPA regulations on potable water quality.

Extensive research on photodegradation of TOrCs is ongoing. Despite this, the most work done focuses on batch reactor systems in which the efficiency of energy is relatively low due to light

losses throughout the system. This can be mitigated using continuous-flow reactor systems that are, in general, more appropriate for large-scale wastewater treatment applications.

This study investigates the photodegradation of TOrCs in both batch and continuous-flow reactor systems. Photodegradation of TOrCs occurs via direct and indirect photolysis mechanisms. Direct photolysis occurs when photons are adsorbed by the TOrC and degraded (Wang et al., 2017). Indirect photolysis occurs when reactive intermediates generated from photosensitizers at an excited-state due to adsorbed radiation react with TOrCs (Wang et al., 2017). Reactive intermediates evaluated include singlet oxygen ($^1O_2$), triplet-state chromophoric dissolved organic matter (^{3}CDOM*), and hydroxide radicals ($^{\bullet}$OH). Batch reactor experiments were meant to determine quantum yields for the direct photolysis of TOrCs. Additional experiments in the batch systems were used to analyze TOrC degradation in reclaimed wastewater, where both direct and indirect photolysis were observed. Using those results, continuous-flow experiments were completed to model the photodegradation of TOrCs in reclaimed wastewater. Continuous-flow reactor experiments and modeling involved both UV-254 nm and UV-185/254 nm lamps.

A comprehensive list of the TOrCs investigated in this study and their uses is summarized in Table 1.

Table 1. Summary of TOrCs Analyzed in this Study

TOrC	Use	Category
Acesulfame K	Sweetener	Personal care product
Atenolol	β-Blocker	Pharmaceutical
Atrazine	Herbicide	Pesticide
Benzophenone	UV blocker	Personal care product
Benzotriazole	Corrosion inhibitor	Industrial compound
Bisphenol A	Plasticizer	Industrial compound
Clofibric acid	Lipid regulator	Pharmaceutical
Dexamethasone	Anti-inflammatory	Pharmaceutical
Diphenhydramine	Antiarrhythmic	Pharmaceutical
Fluoxetine	Anti-depressant	Pharmaceutical
Furosemide	Fluid retention	Pharmaceutical
Hydrochlorothiazide	Antihypertensive	Pharmaceutical
Hydrocortisone	Anti-inflammatory	Hormone
Ibuprofen	Analgesic	Pharmaceutical
Prednisone	Anti-inflammatory	Pharmaceutical
Primidone	Anticonvulsant	Pharmaceutical
Propranolol	β-Blocker	Pharmaceutical
Propyl 4-hydroxybenzoate	Preservative in cosmetics	Personal care product
Propylparaben	Preservative in cosmetics	Personal care product
Simazine	Herbicide	Pesticide
Sulfamethoxazole	Antibiotic	Pharmaceutical

2 MATERIALS & METHODS

2.1 CHEMICALS

Twenty-one analytical grade (≥98%) TOrCs were acquired from Sigma-Aldrich (Table 1). TOrC stock solutions were prepared at concentrations of 2 g L^{-1} in deionized water from a Millipore Milli-Q Advanced Water Purification System (resistivity ≥ 18.0 mΩ cm^{-1}). Hydrogen peroxide (H_2O_2) was obtained from Sigma-Aldrich for actinometry experiments. Sodium azide (≥99.5%) and potassium sorbate (≥99%) were purchased from Sigma Aldrich, and HPLC grade isopropyl alcohol was from OmniSolv for use as reactive radical quenchers. Sodium phosphate monobasic monohydrate (≥98%) was obtained from Sigma-Aldrich, and HPLC grade methanol and acetonitrile were purchased from Fisher Scientific for chromatographic analysis.

2.2 SAMPLE COLLECTION

Ultrafiltration (UF) filtrates and reverse osmosis (RO) concentrates were collected from an UF and RO process at the University of Arizona's Water & Sustainability Technology (WEST) Center in Tucson, Arizona. This system treats up to 75 m^3/d of reclaimed wastewater from Pima County's Agua Nueva Water Reclamation Facility that has undergone tertiary treatment. The water is pumped to the UF system. UF filtrate is further treated via RO membranes allowing permeate and concentrate to be obtained with a recovery rate near 60%. System details and UF filtrate quality data were described by Alhussaini et al. (2024).

2.3 TOC & IC METHODS

Dissolved organic carbon (DOC) measurements were taken using a Total Organic Carbon (TOC) analyzer (Shimadzu TOC-L CSH). Calibration standards were prepared with potassium hydrogen phthalate to determine DOC concentrations. Samples and standards were acidified prior to analysis with hydrochloric acid to pH 3 to remove inorganic carbon.

Anion concentrations including fluoride, chloride, bromide, sulfate, nitrite, nitrate, and phosphate were measured using an ion chromatography (IC) mass spectrometry system (Dionex ICS-500 Ion Pac) with 22 mM potassium hydroxide eluent. Each sample was filtered using 0.45 μm Tisch scientific glass fiber syringe filters. TOC and IC results for filtrate and cocentrate measurements are reported in Table 2.

Table 2. TOC/IC Results Summary

Sample	TOC (mg/L)	F^- (mg/L)	Cl^- (mg/L)	Br^- (mg/L)	SO_4^- (mg/L)	NO_2^- (mg/L)	NO_3^- (mg/L)	PO_4^- (mg/L)
UF filtrate	9.099	0.42 ±0.00	138.4 ±0.68	ND	148.0 ±0.01	20.55 ±0.05	20.55 ±0.05	0.79 ±1.11
Concentrate	13.71	0.64 ±0.00	229.5 ±0.36	ND	279.8 ±0.77	ND	35.42 ±0.07	2.55 ±0.21

2.4 QUANTIFICATION OF TRACE ORGANIC COMPOUNDS

Concentrations of TOrCs were determined using ultra-high performance liquid-chromatography (UHPLC) and ultra-high performance liquid-chromatography-mass spectrometry (LC-MS). UHPLC measurements were quantified by an Agilent 1290 Infinity UHPLC with a 150×4.6 mm Agilent Technologies column. Table 3 provides an overall summary of HPLC methods including mobile phase, flow rate, and retention time utilized for each TOrC in this study.

Table 3. HPLC Detection Method of TOrCs

Analyte	Mobile Phase	Flow Rate	Detection Wavelength	Retention Time
Acesulfame K	(65%) 1% phosphoric acid (35%) acetonitrile	1 mL/min	230 nm	2.4 min
Atenolol	(95%) 2mM PBS acidified with phosphoric acid (pH 3) (5%) acetonitrile	1 mL/min	220 nm	8.7 min
Atrazine	(65%) 1% phosphoric acid (35%) acetonitrile	1 mL/min	220 nm	7.7 min
Benzophenone	(35%) acetonitrile (15%) methanol (45%) DI water	1 mL/min	250 nm	9.5 nm
Benzotriazole	(65%) 1% phosphoric acid (35%) acetonitrile	1 mL/min	260 nm	3.2 min
Bisphenol A	(65%) 1% phosphoric acid (35%) acetonitrile	1 mL/min	215 nm	12.7 min
Clofibric acid	(65%) 1% phosphoric acid (35%) acetonitrile	1 mL/min	220 nm	12.7 min
Dexamethasone	(65%) 1% phosphoric acid (35%) acetonitrile	1 mL/min	240 nm	7.2 min
Diphenhydramine	(65%) 1% phosphoric acid (35%) acetonitrile	1 mL/min	215 nm	4.9 min
Fluoxetine	(65%) 1% phosphoric acid (35%) acetonitrile	1 mL/min	215 nm	8.3 min
Furosemide	(35%) acetonitrile (15%) methanol (45%) DI water	1 mL/min	230 nm	3.9 min
Hydrochlorothiazide	(65%) 1% phosphoric acid (35%) acetonitrile	1 mL/min	220 nm	3.4 nm
Hydrocortisone	(65%) 1% phosphoric acid (35%) acetonitrile	1 mL/min	240 nm	4.7 min
Ibuprofen	(55%) 1% phosphoric acid (45%) acetonitrile	1.2 mL/min	220 nm	6.7 min
Prednisone	(65%) 1% phosphoric acid (35%) acetonitrile	1 mL/min	240 nm	5.6 min
Primidone	(65%) 1% phosphoric acid (35%) acetonitrile	1 mL/min	215 nm	2.9 min
Propranolol	(65%) 1% phosphoric acid (35%) acetonitrile	1 mL/min	215 nm	3.8 min

Propyl 4-hydroxybenzoate	(35%) acetonitrile (15%) methanol (45%) DI water	1 mL/min	260 nm	4.7 min
Propylparaben	(65%) 1% phosphoric acid (35%) acetonitrile	1 mL/min	260 nm	10.1 min
Simazine	(65%) 1% phosphoric acid (35%) acetonitrile	1 mL/min	220 nm	5.6 min
Sulfamethoxazole	(65%) 1% phosphoric acid (35%) acetonitrile	1 mL/min	215 nm	5.2 min

LC-MS methods were formulated according to Anumol & Snyder (2015) with the following modifications. The chromatographic separation was performed in a 2.1×100 mm column and analyzed in an Agilent 6460 triple quadrupole mass spectrometry detector with electrospray ionization (ESI-MS). Separation is performed for an 80 µL injection volume using a 350 µL min^{-1} flow rate of 0.1% acetic acid and 0.1% acetic acid in acetonitrile in a defined gradient over an 18 minute runtime. For the first four minutes, the mobile phase flow will be composed of 5% of the acetic acid in acetonitrile solution, then increased linearly to 100% between 4 and 11 minutes. This is held till 12 minutes then reduced back to 5% at 12.5 minutes where it was maintained for the remainder of the runtime. A Horiba Aqualog Fluorometer was used to measure absorbance of samples from 200–800 nm.

2.5 EXPERIMENTAL SETUP

2.5.1 BATCH REACTOR SYSTEM

Two batch reactor systems were utilized. Both systems were equipped with UV-254 nm lamps from different manufacturers. The first batch system is equipped with a SaniLight D48-2S lamp,

and the second system contained a NeoTech LK-38-D lamp. Open topped glass reactors were filled to an initial volume of 300 mL with TOrC spiked DI water, UF filtrate, or concentrate and positioned 13.0 cm and 43.5 cm below the lamp for the SaniLight and NeoTech reactor systems respectively. Reactor sides were covered by a black cloth to mitigate light interference and continuously stirred throughout the course of the experiment. Sample volumes collected were 6 mL (for HPLC analysis) and 10 mL (for LC-MS analysis) at defined intervals between 0.0 to 240 min. Sampling intervals varied for each TOrC depending on their degradation rates. The experimental setup is shown in Figure 1.

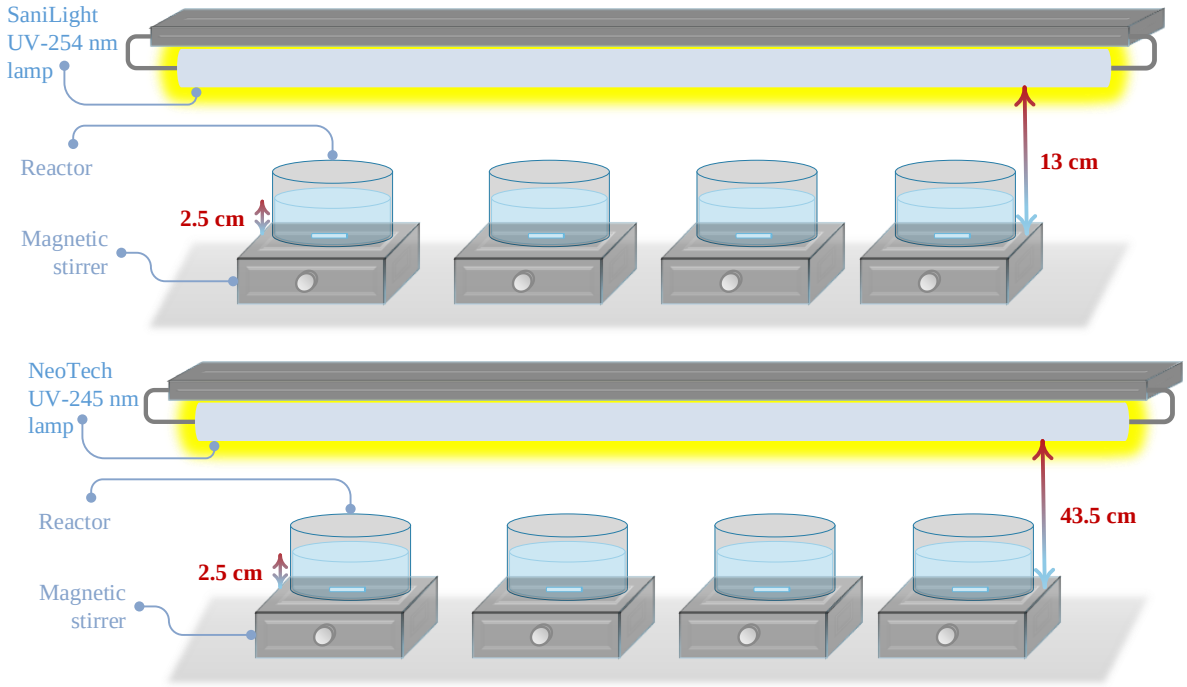

Figure 1. UV-254 nm Batch Reactor System Experimental Setups

2.5.2 CONTINUOUS-FLOW REACTOR SYSTEM

The continuous-flow reactor system in this study consisted of a NeoTech T238 cylindrical chamber reactor equipped with UV-254 nm (NeoTech LK-38-D) or UV-185/254 nm (NeoTech

LK-38) lamps encased centrally in the chamber by a quartz sleeve. The chamber has a pathlength of 0.78 cm across the annular region and a length of 101.4 cm for a volume of up to 825 mL (Figure 2).

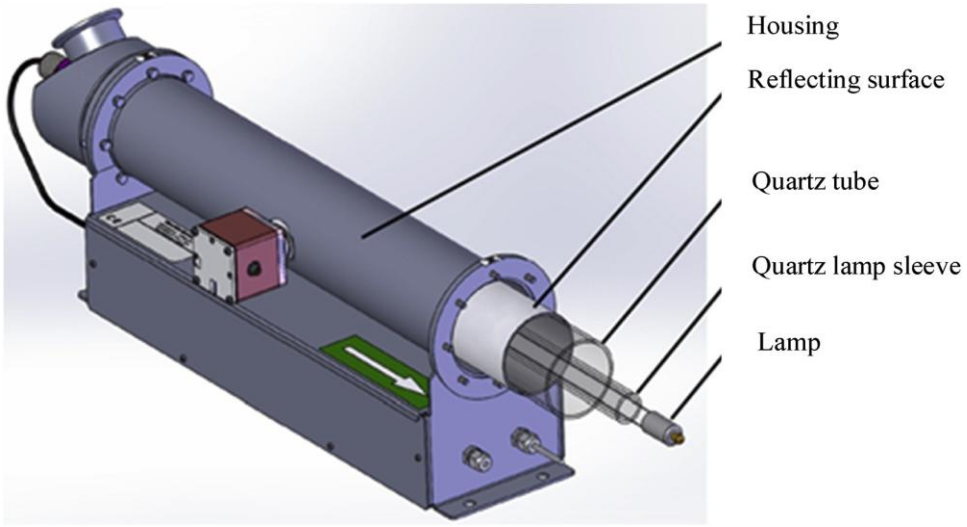

Figure 2. Continuous-Flow Reactor System Configuration (Zhang et al., 2019)

Water was supplied to the reactor via centrifugal pump (Dayton, 4JMV2) from a 90 L feed tank. Continuous-flow experimentation was conducted at flow rates from 0.0 – 6.5 gpm. Flows were measured using a F-400 series Bule-White flow meter to determine outlet concentrations as a function of residence times. The experimental setup of the continuous-flow system is illustrated in Figure 3.

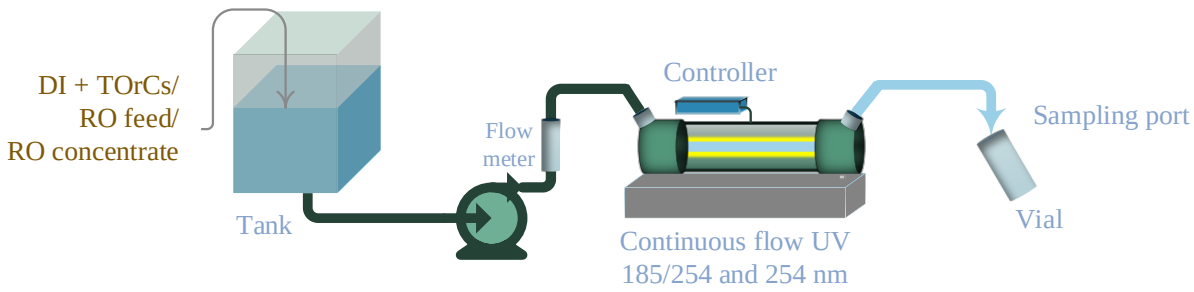

Figure 3. UV-254 nm/UV-185/254 nm Continuous-Flow Reactor Experimental Setup

3 RESULTS & DISSCUSSION

3.1 BATCH REACTOR SYSTEM

The batch reactor system in this study was used to investigate reaction kinetics, determine quantum yields for TOrC transformations, and model TOrC degradation. Actinometry was used to determine light intensity for each setup. Based on TOrC degradations in reclaimed wastewater, further experiments were performed to identify reactive intermediates for TOrCs that experienced indirect photolysis.

3.1.1 **ACTINOMETRY**

Actinometry was completed using 25 mM H_2O_2 to determine the light intensity of the UV-254 nm lamp in each batch reactor system. The photolysis of H_2O_2 follows zeroth-order kinetics given by

$$[H_2O_2] = [H_2O_2]_o - 3\,\Phi_{H_2O_2}\, f_{H_2O_2}\, I_o\, (1 - e^{-2.303\, A_{solution}\, l})\, t \quad (1)$$

where $[H_2O_2]$ is the molar concentration of hydrogen peroxide at time t, $\Phi_{H_2O_2}$ = 0.5 mol/Ein is the moles of H_2O_2 degraded per mole of photons adsorbed, $f_{H_2O_2}$ is the fraction of total light adsorption by H_2O_2, I_o is the incident light intensity, $A_{solution}$ is the absorbance of the solution, and l = 2.5 cm is the pathlength. Incident light intensity was estimated as 2.3E-04 Ein mol^{-1} min^{-1} for the SaniLight lamp and 4.50E-05 Ein mol^{-1} min^{-1} for the NeoTech lamp. Figure 4 illustrates actinometry modeling used to determine the incident light intensity for the NeoTech lamp system.

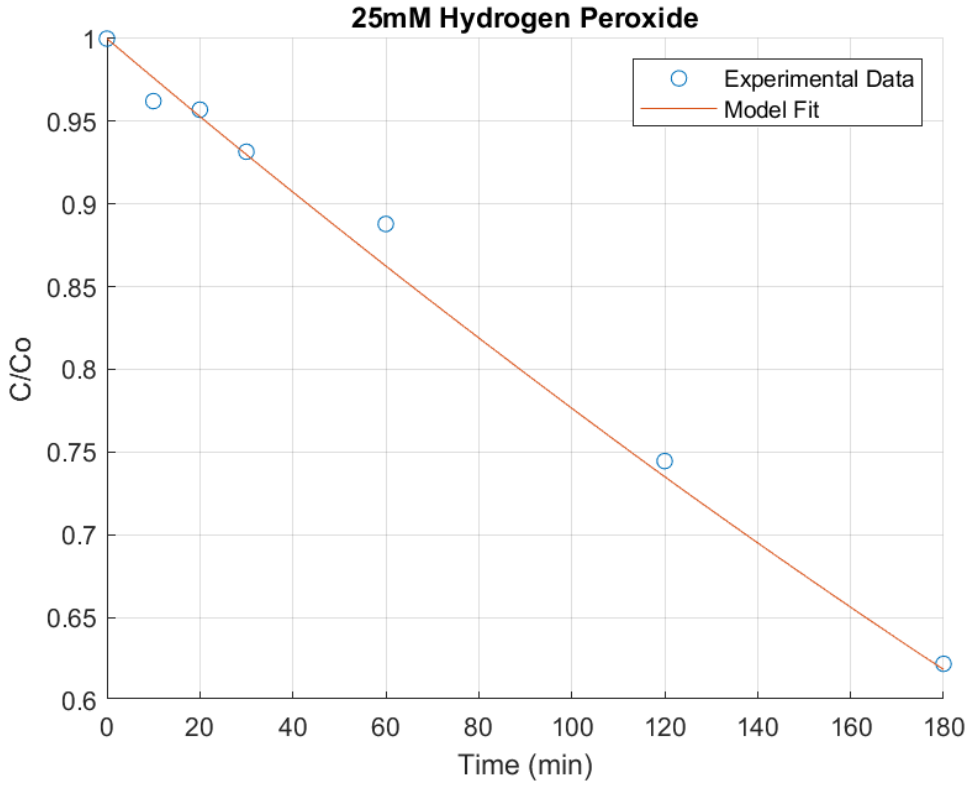

Figure 4. Photodegradation of 25 mM H_2O_2 in UV-254 nm Batch Reactor System

3.1.2 QUANTUM YIELD OF TRACE ORGANICS

The quantum yields of the TOrCs were independently estimated by spiking 25 µM of a given TOrC in DI water and modeling the direct photolysis using the kinetic expression

$$\frac{d[\mathrm{TOrC}]}{dt} = -\Phi_{\mathrm{TOrC}}\, f_{\mathrm{TOrC}}\, I_o\, (1 - e^{-2.303\, A_{\mathrm{solution}}\, l}) \qquad (2)$$

where [TOrC] is the time-dependent molar concentration of the TOrC, Φ_{TOrC} is the moles of TOrC degraded per mole of photon adsorbed (quantum yield), f_{TOrC} is the fraction of total adsorbed light by the TOrC, A_{solution} is the absorbance of the solution, and l = 2.5 cm is the pathlength. The fraction of total light adsorbed by the TOrC is calculated by

$$f_{TOrC} = \frac{\varepsilon_{254}\,[TOrC]}{A_{solution}} \quad (3)$$

where ε_{254} is the TOrC-specific molar adsorption coefficient. Solutions containing individual TOrCs were prepared at three different concentrations to determine an average molar adsorption coefficient at 254 nm. Each value was calculated according to the Beer-Lambert law

$$A_{254} = \frac{\varepsilon_{254}\,[TOrC]\,l}{MW} \rightarrow \varepsilon_{254} = \frac{A_{254}MW}{[TOrC]\,l} \quad (4)$$

where l = 1 cm represents the pathlength of the spectrophotometer and MW is the molecular weight of the TOrC. Table 4 provides a summary of the average molar adsorption coefficient determined here for each TOrC in this study and values found in previous literature. ND signifies values that were not determined.

Table 4. Summary of Molar Adsorption Coefficients for TOrCs

TorC	ε_{254} (M^{-1} cm^{-1})		
	This Study	(Yu et al., 2019)	(Xu & Huang, 2023)
Acesulfame K	2661	3600	ND
Atenolol	859	300	352
Atrazine	5546	3400	3268
Benzophenone	19373	16200	ND
Benzotriazole	8272	5600	ND
Bisphenol A	1344	1000	679
Clofibric acid	406	300	263
Dexamethasone	9597	ND	ND
Diphenhydramine	362	300	ND
Fluoxetine	934	600	ND
Furosemide	8226	ND	ND
Hydrochlorothiazide	9022	5900	ND
Hydrocortisone	9490	14400	ND
Ibuprofen	384	300	399
Prednisone	12919	13100	ND
Primidone	277	200	ND

Propranolol	1981	1200	ND
Propyl 4-hydroxybenzoate	13245	ND	ND
Propylparaben	14550	7400	ND
Simazine	1287	600	2870
Sulfamethoxazole	17466	16500	16015

Direct photodegradation modeling (equation 2) was modified to consider a changes in solution absorbance over time allowing for a numerical approach to estimate quantum yields for each TOrC. Estimated quantum yields for TOrCs determined in this study are summarized in Table 5 along with previously published values. ND signifies values that were not determined.

Table 5. Summary of Quantum Yield for TOrCs

TorC	**Φ_{254} (mol E_{in}^{-1})**		
	in this study	**(Yu et al., 2019)**	**(Xu & Huang, 2023)**
Acesulfame K	0.45	0.187	ND
Atenolol	0.0035	0.089	0.0186
Atrazine	0.053	0.036	0.0498
Benzophenone	0.007	0.002	ND
Benzotriazole	0.012	0.013	ND
Bisphenol A	0.0045	0.056	0.01
Clofibric acid	0.65	0.467	0.788
Dexamethasone	0.75	ND	ND
Diphenhydramine	0.092	0.121	ND
Fluoxetine	0.44	0.363	ND
Furosemide	0.015	ND	ND
Hydrochlorothiazide	0.35	0.01	ND
Hydrocortisone	0.055	0.022	ND
Ibuprofen	0.04	0.035	0.0712
Prednisone	0.95	0.069	ND
Primidone	0.27	0.116	ND
Propranolol	0.0021	0.009	ND
Propyl 4-hydroxybenzoate	0.00032	ND	ND
Propylparaben	0.0029	0.004	ND
Simazine	0.2	0.217	0.0556
Sulfamethoxazole	0.27	0.058	0.0445

The quantum yields determined here and from literature (Table 5) have many discrepancies. These differences may be attributed to differences in quantification methodology, initial TorC concentrations, temperature, and pH. Nevertheless, quantum yields obtained have yielded strong modeling fits to experimental data (Figure 5).

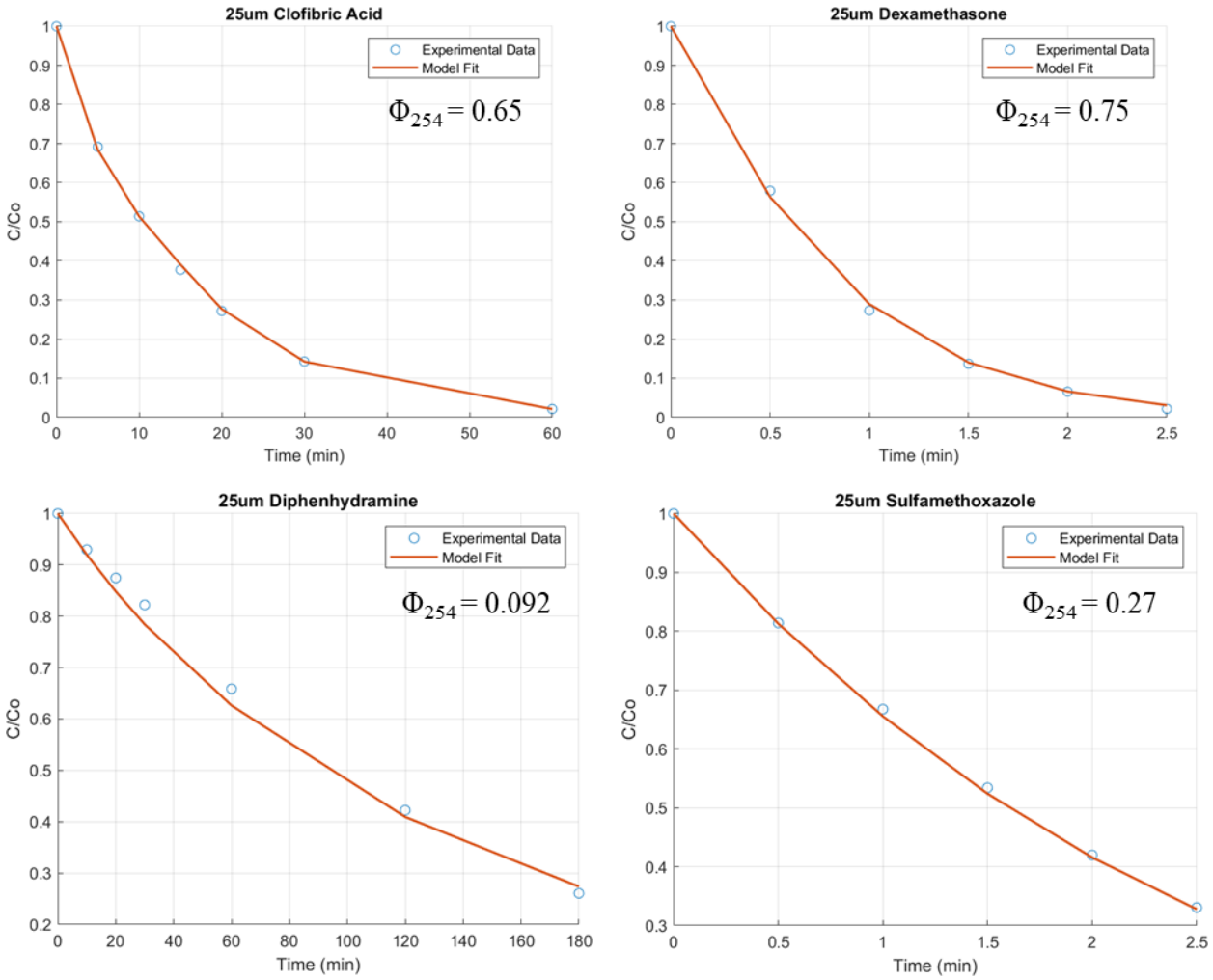

Figure 5. Photodegradation of TOrCs using UV-254 nm Batch Reactor System

3.1.3 MODELING PHOTODEGREDATION IN RECLAIMED WASTEWATER

Batch reactor TOrC photodegradation experiments were carried out in DI water, UF filtrates, and concentrates. Experimental results appeared to support quantum yields determined via direct photolysis of TOrCs in DI water for prediction of TOrC degradation in UF filtrates and concentrates. Since the UF filtrates and concentrates contain additional concentrations of many other species, a screening effect was expected to occur due to light absorption by other compounds. For the majority of the TOrCs, this was obtained and higher adsorption values are necessary to accurately represented light screening effects within the model. The effects of shading (λ = 254 nm) are apparent in the photodegradation of 25 µM dexamethasone well represented by the model when shading is accounted for in Figure 6.

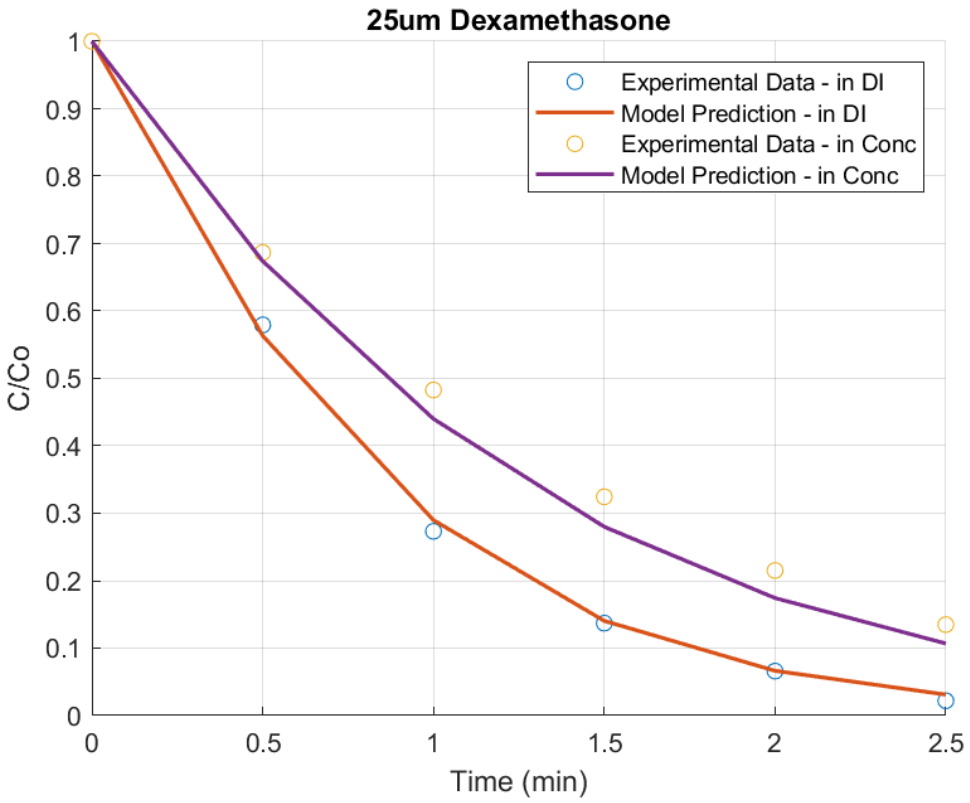

Figure 6. Photodegradation of 25 µM Dexamethasone in DI water vs Concentrate using UV-254 nm in Batch Reactor System

Accelerated degradation of atenolol and diphenhydramine were observed in UF filtrate and concentrate than in DI water. Results suggest that although UF filtrate and concentrate slow photodegradation due to light screening, atenolol and diphenhydramine were determined to undergo both direct and indirect photolysis, reacting with reactive intermediates formed via light-driven pathways in UF filtrate and concentrate. Degradation by indirect photolysis can be modeled by

$$\frac{d[\mathrm{TOrC}]}{d\mathrm{t}} = -\mathrm{k_{RI}}\,[\mathrm{RI}][\mathrm{TOrC}] \quad (5)$$

where [RI] is the molar concentration of the reactive intermediate and k_{RI} is the rate coefficient of the reactive intermediate. This can be combined with the model for direct photolysis (Equation 2) to derive an overall model accounting for both direct and indirect photolysis as given by

$$\frac{d[\mathrm{TOrC}]}{d\mathrm{t}} = -\Phi_{\mathrm{TOrC}}\,\mathrm{f_{TOrC}}\,\mathrm{I_o}\,(1-\mathrm{e}^{-2.303\,\mathrm{A_{solution}}\,l}) - \mathrm{k_{RI}}\,[\mathrm{RI}][\mathrm{TOrC}]. \quad (6)$$

Using the quantum yield determined for direct photolysis, an observed reaction rate (k_{obs}) where

$$\mathrm{k_{obs}} = \mathrm{k_{RI}}\,[\mathrm{RI}] \quad (7)$$

is determined to accurately model photodegradation by direct and indirect photolysis. Figure 7 shows the degradation of 25 μM diphenhydramine through direct photolysis in DI water and indirect photolysis in UF filtrate where k_{obs} is 0.019 mol L^{-1} min^{-1}.

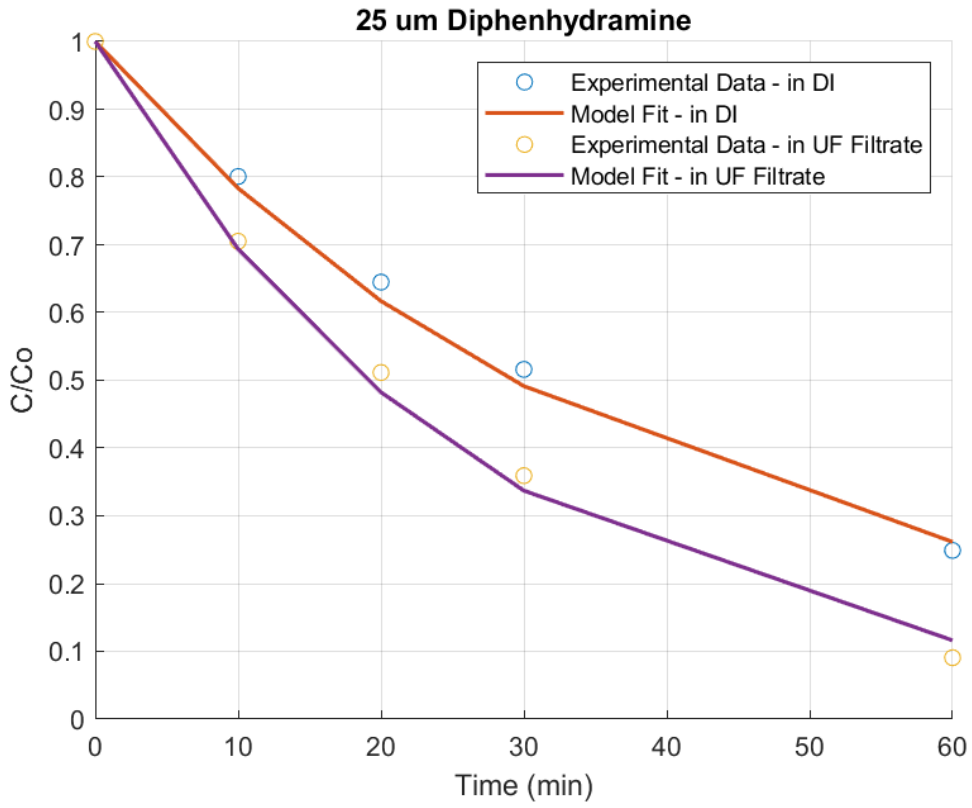

Figure 7. Photodegradation of 25 µM Diphenhydramine in DI water vs UF filtrate using UV-254 nm in Batch Reactor System

3.1.4 IDENTIFICATION OF REACTIVE INTERMEDIATES

Following observations of the indirect photolysis of diphenhydramine and atenolol in reclaimed wastewater (UF filtrate or concentrate), experiments were completed using three quenchers. The purpose was to identify reactive intermediates involved in the indirect photolysis of those TOrCs. Each quencher tested is reactive with a different intermediates, so specific reactive intermediates can be identified based on which quencher effectively inhibits the rate of degradation of diphenhydramine and atenolol in UF filtrate or concentrate. Sodium azide (NaN_3) was used as a quencher of singlet oxygen ($^1O_2$) (Qian et al., 2014). Based on the data shown in Figure 8 (with and without NaN_3), NaN_3 was not effective in quenching the indirect photolysis reaction of

diphenhydramine. Therefore, singlet oxygen is not the reactive intermediate responsible for observed indirect photolysis.

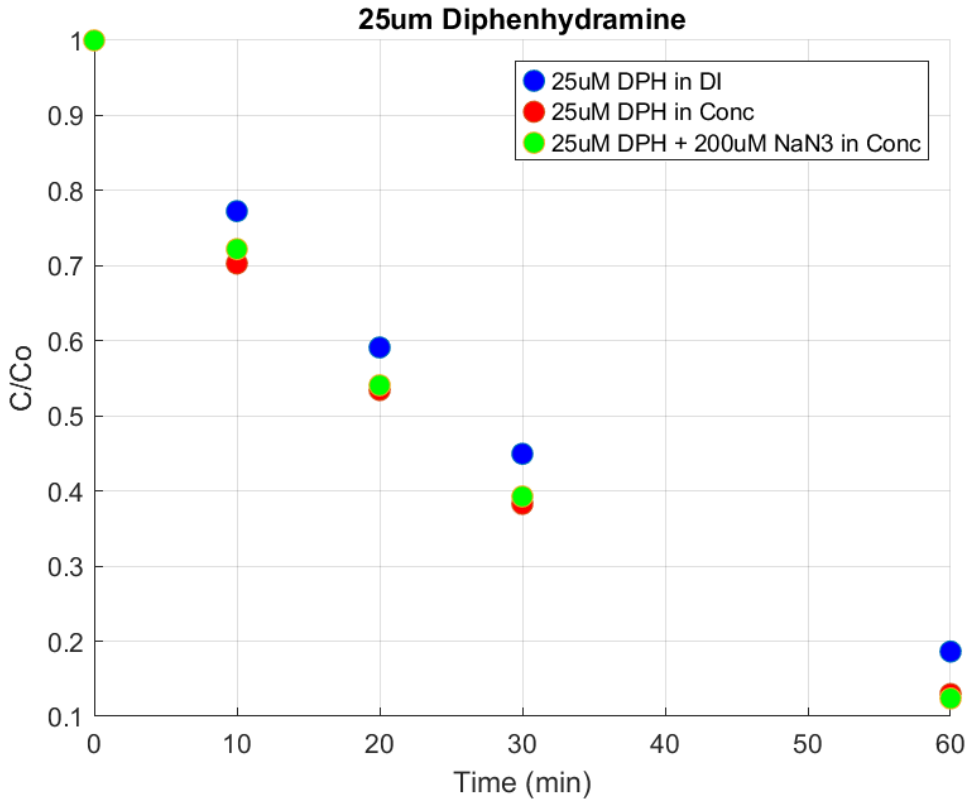

Figure 8. Photodegradation of 25 µM Diphenhydramine in the Presence and Absence of Sodium Azide, an inhibitor of Indirect Photolysis Pathways Involving Formation of Singlet Oxygen

Sorbate (HDA) was used to test for the presence of triplet-state chromophoric dissolved organic matter (^{3}CDOM*) (Moor et al., 2019). Figure 9 data indicates that light screening was more relevant to interference with ^{3}CDOM* photolysis than was than the quenching of ^{3}CDOM* by HDA.

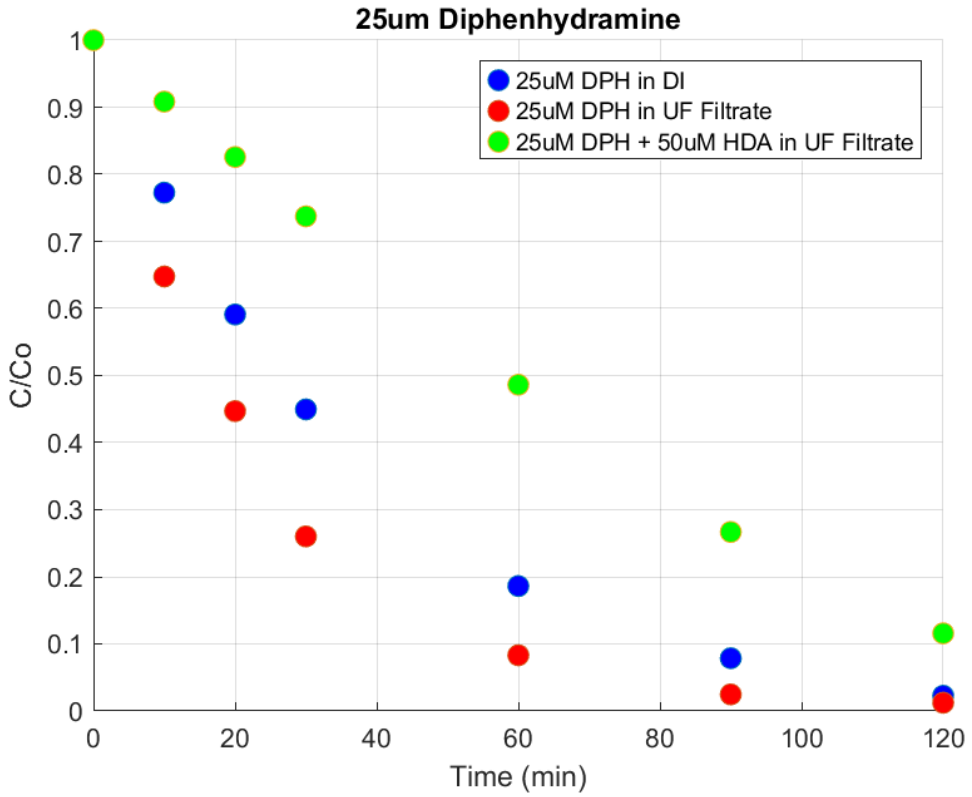

Figure 9. Photodegradation of 25 µM Diphenhydramine in the Presence and Absence of Sorbate, an inhibitor of Indirect Photolysis Pathways Involving Formation of Triplet-State Chromophoric Dissolved Organic Matter

The final quencher tested was isopropyl alcohol (IPA), an active quencher of hydroxide radicals (•OH) when present as a reactive intermediate (Qian et al., 2014). The results displayed in Figure 10 show IPA as a potententially effective quencher for the reaction, however, these results are inconclusive.

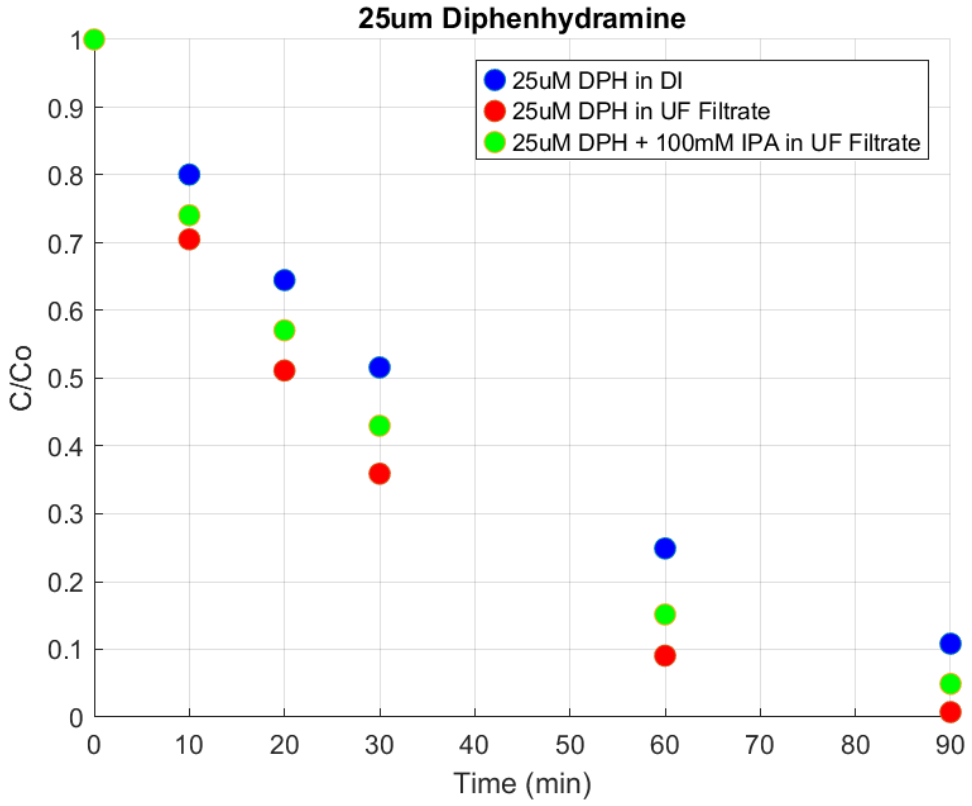

Figure 10. Photodegradation of 25 µM Diphenhydramine in the Presence and Absence of Isopropyl Alcohol, an inhibitor of Indirect Photolysis Pathways Involving Formation of Hydroxide Radicals

Since IPA was added at high concentration to low concentration diphenhydramine, the quenching effect appears smaller than expected given the presence of hydroxide radicals as reactive intermediates. Therefore, the indirect photolyis of diphenhydramine and atenolol cannot be conclusively attributed to the presence of hydroxide radicals as reactive intermediates in the reclaimed wastewater and further exerimentation is required.

3.2 CONTINUOUS-FLOW REACTOR

A continuous-flow reactor system was used to model the degradation of TOrCs under UV-254 nm and UV-185/254 nm irradiation. Light intensity needed for modeling was determined via actonometry.

3.2.1 ACTINOMETRY

Actinometry for the continuous-flow reactor systems used parameter fitting on the disappearance of H_2O_2 to determine the light intensity of the UV-254 nm lamps. Here, 50 mM H_2O_2 was added to the continuous-flow systems, as opposed to the 25 mM H_2O_2 concentration used for the batch systems, to ensure total incident light absorption and eliminate the effect of reflection from the reactor surface. The photolysis of H_2O_2 was assumed to follow the same zeroth-order kinetics given by Equation 1. Incident light intensity was estimated as 1.36E-04 Ein L^{-1} s^{-1} for the UV-254 nm lamp and 1.30E-10 Ein L^{-1} s^{-1} for the UV-185/254 nm lamp. Figure 11 illustrates the actinometry modeling used for determining the incident light intensity for the UV-254 nm lamp.

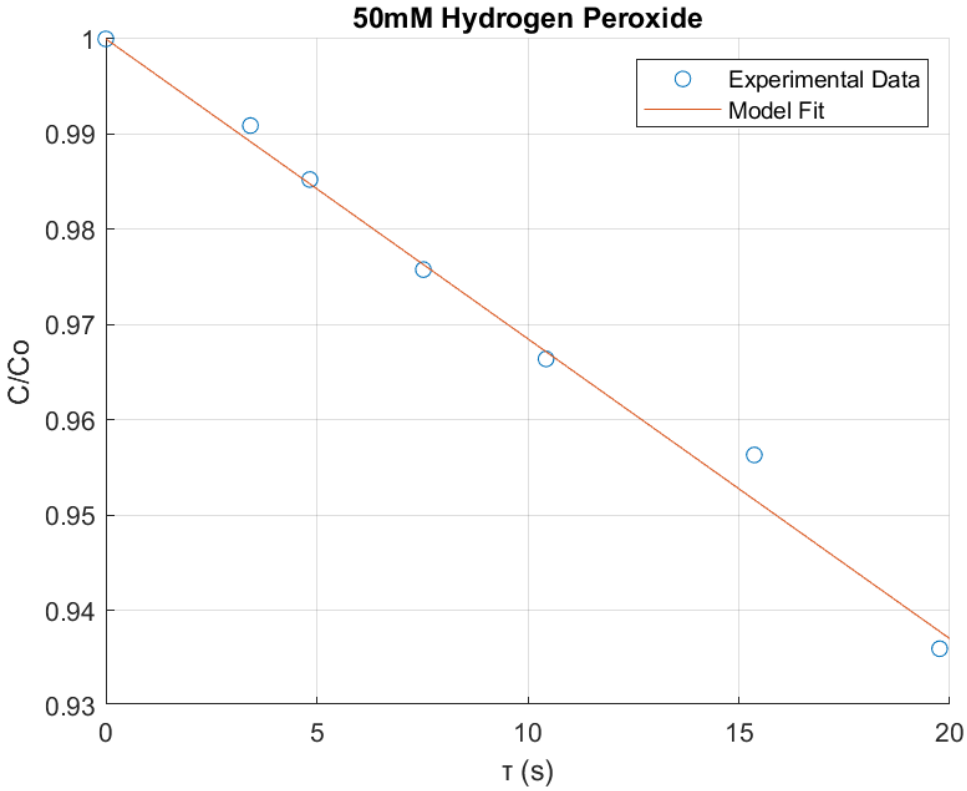

Figure 11. Photodegradation of 50 mM H_2O_2 in UV-254 nm Continuous-Flow Reactor System

Although actinometry was carried out at high initial concentrations to minimize the effect of reflection from the reactor surface, TOrC photodegradation experiments were performed using solutions with relatively high transmittance. To account for the light loss due to reflection in the quartz sleeve, a fitted parameter of $\beta = 0.15$ was used. This value represents a 15% loss of light upon outer surface reflection as determined by previous work completed on this reactor system using high transmittance solutions (Zhang et al., 2019).

3.2.2 MODELING PHOTDEGREDATION IN RECLAIMED WASTEWATER

Photodegradation kinetics in the batch reactor system were used to model the continuous-flow reactor system. As in the batch system, experimentation was performed to determine TOrC degradation in DI water, UF filtrate, and concentrate. Results showed that all TOrCs studied, including atenolol and diphenhydramine, degraded faster in DI water than in UF filtrate or concentrate, emphasizing the dominant effect of direct photolysis over indirect photolysis in the continuous-flow reactor. Photodegradation of TOrCs through direct photolysis in a continuous reactor system is given by

$$\frac{d[TOrC]}{dt} = -\Phi_{TOrC} f_{TOrC}\, I_o \frac{1-e^{-2*2.303*A_{solution} l}}{1-(1-\beta)e^{-2*2.303*A_{solution} l}} \quad (8)$$

where l = 0.78 cm is the pathlength and β = 0.15 is the fraction of light lost by reflection. Based on model application, TOrCs were degraded primarily by direct photolysis under UV-254 nm irradiation in reclaimed wastewater. Therefore, light screening was the dominant effect for the degradation rate of all twenty-one TOrCs studied in reclaimed wastewater. These results are indicated by degradations of 25 μM diphenhydramine in DI water and UF filtrate (Figure 12).

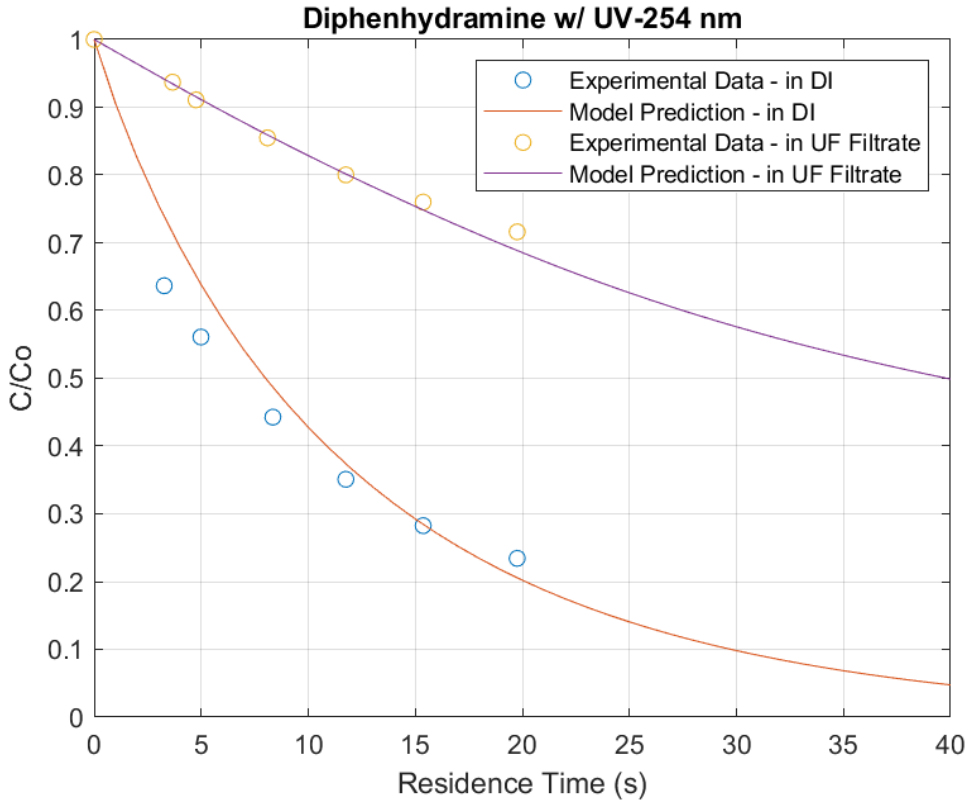

Figure 12. Direct Photodegradation of 25 µM Diphenhydramine in DI water vs UF filtrate using UV-254 nm in Continuous-Flow Reactor System

Further experimentation was performed using the continuous-flow process to evaluate the changes in the degradation of TOrCs in reclaimed wastewater using a UV-254 nm lamp versus a UV-185/254 nm lamp. Similar trends were observed using the UV-185/254 nm lamp i.e., faster TOrC degradation in DI water than in UF filtrate or concentrate due to screening effects. However, it was further observed that all twenty-one TOrCs tested, degraded faster using the UV-185/254 nm lamp than the UV-254 nm lamp in DI water, UF filtrate, and concentrate. This trend is shown for diphenhydramine in DI water (Figure 13).

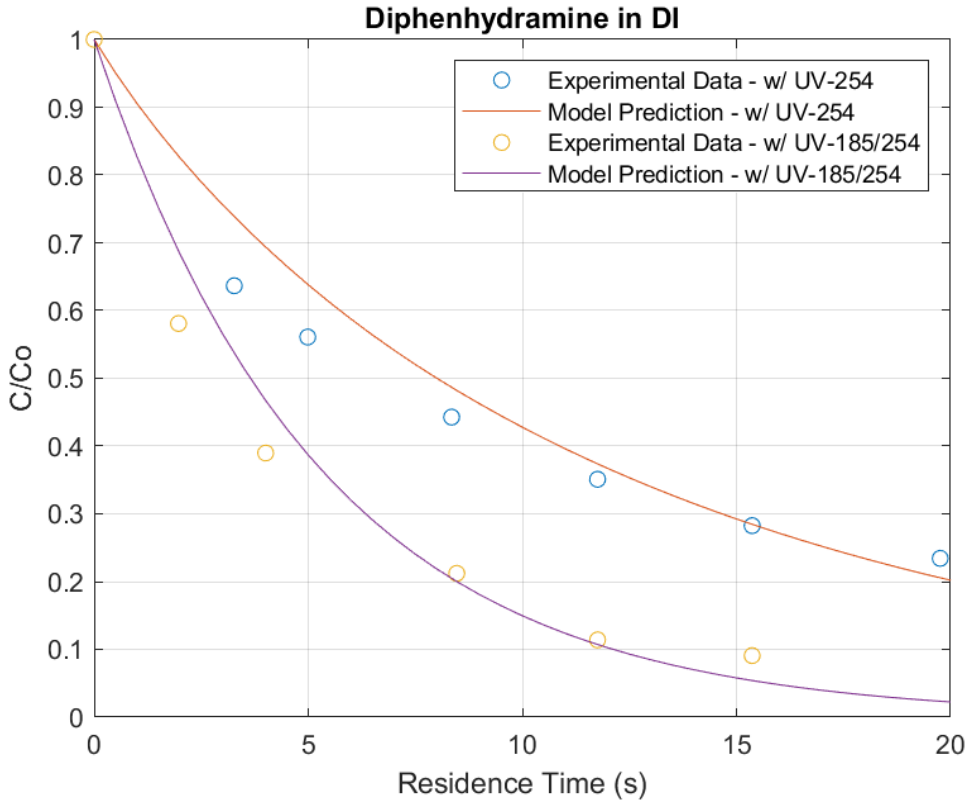

Figure 13. Photodegradation of 25 µM Diphenhydramine in DI water using UV-254 nm vs UV-185/254 nm in Continuous-Flow Reactor System

This can be explained by UV-185 nm driven production of hydroxide radicals per

$$H_2O + h\nu(< 190\ nm) \rightarrow HO^{\bullet} + H^{\bullet} \quad (9)$$

and

$$H_2O + h\nu(< 190\ nm) \rightarrow HO^{\bullet} + H^{\bullet} + e^{\bullet -} \quad (10)$$

that increases the rate of TOrC degradation via indirect photolysis (Zhang, 2019). Degradation from direct and indirect photolysis in a continuous-flow reactor system was given by

$$\frac{d[\mathrm{TOrC}]}{dt} = -\Phi_{\mathrm{TOrC}} f_{\mathrm{TOrC}}\, I_o \frac{1-e^{-2*2.303*A_{solution}l}}{1-(1-\beta)e^{-2*2.303*A_{solution}l}} - k_{RI}[RI][\mathrm{TOrC}]. \quad (11)$$

The k_{obs} for the indirect photolysis of 25 µM diphenhydramine in DI water was 0.19 mol L^{-1} s^{-1} using UV-185/254 nm.

Despite increased degradation rates via indirect photolysis from 185 nm light, screening effects still decrease TOrC degradation in UF filtrate and concentrate. Figure 14 illustrates the increased rate of diphenhydramine degradation by the UV-185/254 nm lamp in comparison to the UV-254 nm lamp for the photodegradation diphenhydramine in reclaimed wastewater. The k_{obs} for the indirect photolysis of diphenhydramine in concentrate using the UV-185/254 nm lamp was 0.25 mol L^{-1} s^{-1}.

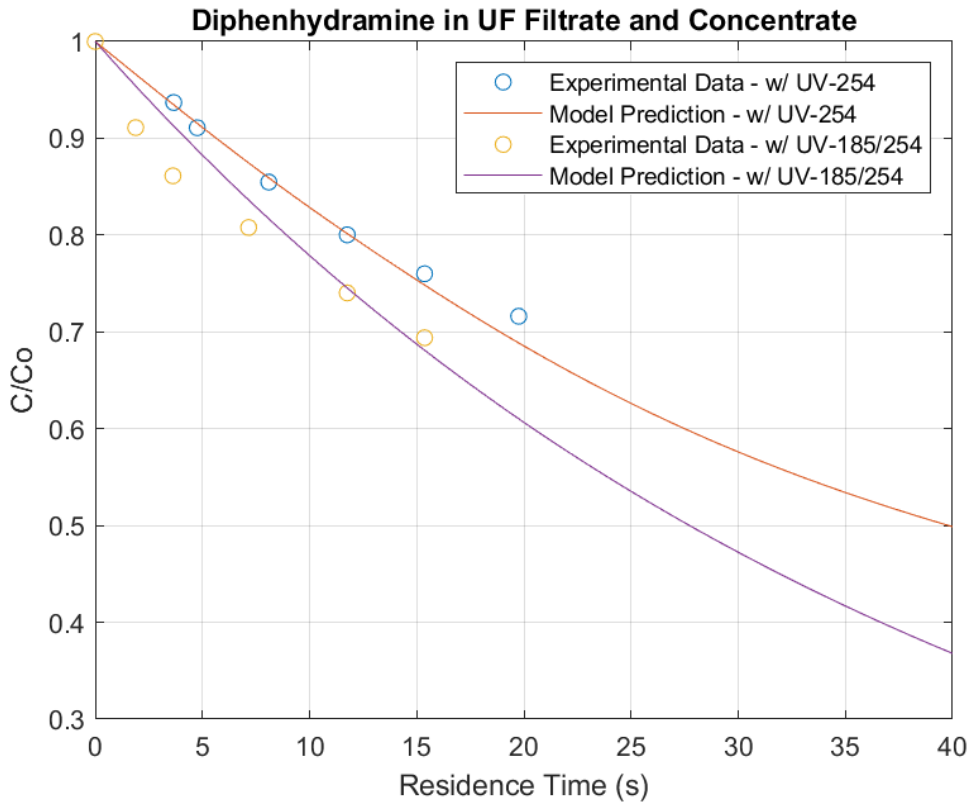

Figure 14. Photodegradation of 25 µM Diphenhydramine in UF filtrate and Concentrate using UV-254 nm vs UV-185/254 nm in Continuous-Flow Reactor System

4 CONCLUSIONS

The kinetics for photodegradation of twenty-one TOrCs under UV-254 nm and UV-185/254 nm irradiation was investigated in an effort to model degradation in both batch and continuous-flow processes. Quantum yield values were deciphered for each TOrC in the study. These values can be used to model TOrC degradation in batch and continuous-flow reactors systems accounting for both direct and indirect photolysis. Atenolol and diphenhydramine experience indirect photolysis in reclaimed wastewater under UV-254 nm irradiation due to the creation of reactive intermediates. These intermediates could be hydroxide radicals, but further experimentation is necessary for this to be conclusive. The indirect photolysis of diphenhydramine and atenolol resulted in a faster degradation in reclaimed water than in DI water within batch reactor system. All other TOrCs degraded faster in DI water than reclaimed wastewater since dissolved compounds remaining in the reclaimed wastewater provided a screening effect. All twenty-one TOrCs degraded faster in DI water than reclaimed wastewater in the continuous-flow system indicating that the screening effect of reclaimed wastewater exceeds that of indirect photolysis in the continuous-flow system. TOrC degradation in the continuous-flow reactor system using the UV-185/254 nm lamp followed a similar trend as continuous-flow using the UV-254 nm lamp in relation to the relative degradation rates of each compound in DI water versus reclaimed wastewater. Degradation using UV-185/254 nm was faster than UV-254 nm for all TOrCs due to indirect photolysis from hydroxide radicals formed by 185 nm being adsorbed and degraded by water.

Further research could be done to conclusively identify reactive intermediated facilitating indirect photolysis for atenolol and diphenhydramine in batch reactor systems. Work could also be done to investigate and model degradation using different continuous-flow reactor geometries.

REFERENCES

Alhussaini, M. A., Souza-Chaves, B. M., Felix, V., & Achilli, A. (2024). Comparative analysis of reverse osmosis for the removal of dissolved contaminant in water reuse applications. Desalination, 586, 117822. https://doi.org/10.1016/j.desal.2024.117822

Anumol, T., & Snyder, S. A. (2015). Rapid analysis of trace organic compounds in water by automated online solid-phase extraction coupled to liquid chromatography–tandem mass spectrometry. Talanta, 132, 77–86. https://doi.org/10.1016/j.talanta.2014.08.011

Castro-Lindarte, L. (2025). USGS releases a comprehensive look at water resources in the United States. U. S. Geological Survey. https://www.usgs.gov/news/national-news-release/usgs-releases-a-comprehensive-look-water-resources-united-states

IPCC (Intergovernmental Panel on Climate Change). 2023: Summary for Policymakers. H. Lee and J. Romero (eds.), Climate Change 2023: Synthesis Report. Contribution of Working Groups I, II and III to the Sixth Assessment Report of the Intergovernmental Panel on Climate Change. Geneva, IPCC, pp. 1–34. www.ipcc.ch/report/ar6/syr/downloads/report/IPCC_AR6_SYR_SPM.pdf.

Miklos, D. B., Remy, C., Jekel, M., Linden, K. G., Drewes, J. E., & Hübner, U. (2018). Evaluation of advanced oxidation processes for water and wastewater treatment – A critical review. *Water Research*, *139*, 118–131. https://doi.org/10.1016/j.watres.2018.03.042

Moor, K. J., Schmitt, M., Erickson, P. R., McNeill, K. (2019). Sorbate as a Triplet-Probe: Triplet Energy and Reactivity with Triplet-State Dissolved Organic Matter via $^1O_2$ Phosphorescence. Environmental Science & Technology, 53, 14, 8078-8086. https://pubs.acs.org/doi/10.1021/acs.est.9b01787

Qian, Y., Yin, X., Lin, H., Rao, B., Brooks, S.C., Liang, L., Gu, B. (2014). Why Dissolved Organic Matter Enhances Photodegradation of Methylmercury. Environmental Science & Technology Letters, 1, 10, 426-431. https://pubs.acs.org/doi/10.1021/ez500254z

Wang, Y., Roddick, F. A., Fan, L. (2017). Direct and indirect photolysis of seven micropollutants in secondary effluent from a wastewater lagoon. Chemosphere, 185, 297-308. https://doi.org/10.1016/j.chemosphere.2017.06.122

Wie, L., Jain, T., Ishida, K., & Liu, H. (2016). A mechanistic understanding of the degradation of trace organic contaminants by UV/hydrogen peroxide, UV/persulfate and UV/free

chlorine for water reuse. Environmental Science: Water Research & Technology, 3, 128-138. https://doi.org/10.1039/C6EW00242K

Xu, J., & Huang, C.-H. (2023). Enhanced Direct Photolysis of Organic Micropollutants by Far-UVC Light at 222 nm from KrCl* Excilamps. Environmental Science & Technology Letters, 10(6), 543–548. https://doi.org/10.1021/acs.estlett.3c00313

Yu, H.-W., Park, M., Wu, S., Lopez, I. J., Ji, W., Scheideler, J., & Snyder, S. A. (2019). Strategies for selecting indicator compounds to assess attenuation of emerging contaminants during UV advanced oxidation processes. Water Research, 166, 115030. https://doi.org/10.1016/j.watres.2019.115030

Zhang, T., Márquez-Hernández, L. I., Arnold, R. G., Diefenthal, G., & Sáez, A. E. (2019). Modeling the UV/H2O2 oxidation of phenolic compounds in a continuous-flow reactor with reflective walls. Journal of Environmental Chemical Engineering, 7(3), 103150. https://doi.org/10.1016/j.jece.2019.103150